Terraced Hollow Oxide Pyramids

Guangwen Zhou,[1,*] William S. Slaughter,[2] and Judith C. Yang[1]

[1]*Department of Materials Science and Engineering, University of Pittsburgh, Pittsburgh, Pennsylvania 15261, USA*
[2]*Department of Mechanical Engineering, University of Pittsburgh, Pittsburgh, Pennsylvania 15261, USA*

(Received 14 February 2005; published 20 June 2005)

We report *in situ* transmission electron microscope dynamic observations of the growth of Cu_2O islands during oxidation of (001)Cu thin films at ~900 °C, which show that the oxide islands have an initially square shape that transits to a terraced pyramid morphology as growth proceeds. The surface topology obtained from *ex situ* atomic force microscopy observation indicates that the terraced oxide pyramids have a hollow structure. A simple mechanical mechanism based on elastic-plastic deformation is proposed to explain the formation of this completely new oxide structure.

DOI: 10.1103/PhysRevLett.94.246101 PACS numbers: 81.16.Pr, 62.25.+g, 68.37.Lp, 81.65.Mq

It has been recognized for a long time that the oxidation of metal surfaces results in the generation of stresses [1,2]. Generally, a few major types of stresses can be distinguished. The first type is epitaxial stresses resulting from phase transformations in the oxide and/or in the metal subsurface zone. The second is geometrically induced stresses that result from volume change that accompanies the conversion of metal into oxide. The other type includes the so-called intrinsic growth stresses, which arise when new oxide is formed within the already existing oxide, and, last, thermal-expansion mismatch stresses. In the growth of bulk oxide during metal oxidation, the relief of these stresses may occur by fracture in the oxide scale and/or in the underlying metals, or by separation of the oxide-metal interface. However, as the dimension of materials approaches nanoscale, the generation and relaxation of stresses during oxidation may be much different from the corresponding bulk materials. These alternate pathways may provide unique opportunities for creation of nanoscale oxide structures and provide a variety of technological opportunities via exploitation of potentially novel optical, magnetic, sensor, and catalytic properties of these oxide islands [3,4]. We have therefore investigated the effects of the generation and relaxation of stress on the formation of oxide nanostructures by choosing Cu thin film as a model system. It is based on the generation of volume-constraint stress by oxidizing Cu($a = 3.61$ Å) to Cu_2O($a = 4.217$ Å) at ~900 °C, this temperature provides very fast oxidation kinetics, and, therefore, fast stress buildup in the oxide. Our experiments involve *in situ* oxidation of (001)Cu thin films by using an environmental transmission electron microscope (TEM), which provides interesting dynamic details of the stress generation and relaxation in growing oxide islands by observing their size and shape evolution. The present results demonstrate that controlled oxidation is an efficient approach to create novel oxide nanostructures.

Our experiments were carried out in a modified JEOL 200CX TEM chamber with base pressure of $\sim 10^{-8}$ torr [5]. Oxygen gas (99.999% purity) can be admitted into the microscope to oxidize the sample at a pressure between 5×10^{-5} Torr and 760 Torr. Real time observation can be made at pressures $\leq 8 \times 10^{-4}$ Torr. The specially designed sample holder allows for resistive heating up to 1000 °C. Single crystal (001)Cu films were grown on irradiated (001)NaCl substrates in an ultrahigh vacuum (UHV) *e*-beam evaporation system, then removed from the substrate by dissolving the NaCl in deionized water. The native Cu oxide was removed by annealing the Cu films in the TEM under vacuum conditions at ~800 °C [6].

Figure 1(a) shows the typical morphology of Cu_2O pyramids during oxidation of (001)Cu film at 900 °C. The pyramids are faceted with terraces and ledges. In order to visualize the growth of one island without interference due to coalescence with neighboring pyramids, the Cu film is oxidized at a lower oxygen pressure of 3×10^{-4} Torr. The morphology evolution of a pyramid is recorded, as shown in Fig. 1(b). Oxidation of the Cu thin film begins rapidly and oxide nuclei are seen on the surface within a few seconds after introduction of oxygen gas into the microscope, as followed by lateral growth. The terraces and ledges appear one by one as growth proceeds. This *in situ* observation revealed that the oxide growth occurs only along the pyramid perimeter, and the pyramid thickening is caused by progressive formation of new ledges and terraces on the base terrace.

The microstructure in the Cu_2O/Cu interface area is analyzed by TEM. Figure 2(a) shows a Cu_2O pyramid and (b) is a dark-field (DF) TEM image from the Cu/Cu_2O interface region, where the Cu thickness fringes are visible. Figure 2(c) is the diffraction pattern from the interface region, which gives their cube-on-cube relationship at the interface. Figure 2(e) is a high-resolution electron microscopy (HREM) image from the interface, where Moiré fringes are visible caused by the overlap of Cu and Cu_2O lattices. HREM images of Cu near the interface reveal that the Cu lattice appears undistorted with no strain as shown in Fig. 2(d), but a lot of lattice distortions occur in the oxide near the interface, as shown in Fig. 2(f). Occurrence of Moiré fringes only at the interface area

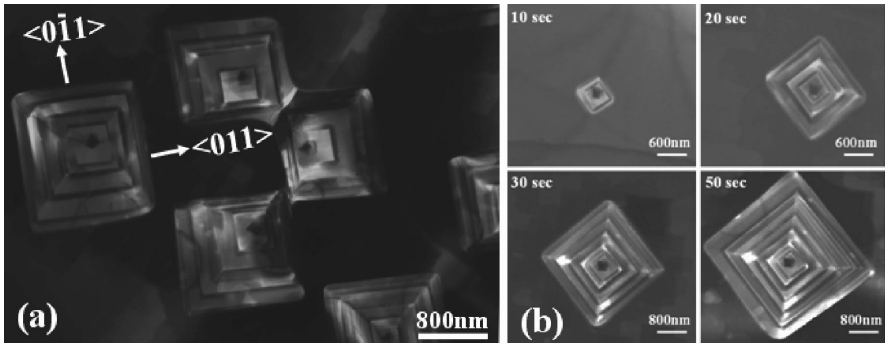

FIG. 1. (a) Typical morphology of Cu_2O terraced pyramids formed during oxidation of (001)Cu thin film (70 nm in thickness) at 900 °C in $pO_2 = 5 \times 10^{-4}$ Torr. (b) *In situ* TEM observation of the growth of a Cu_2O pyramid at 900 °C in $pO_2 = 3 \times 10^{-4}$ Torr.

suggests that the oxide completely penetrates through the Cu film with an inclined interface, which is determined to be $(111)Cu_2O/(111)Cu$ based on the cube-on-cube Cu_2O/Cu orientation and the inclined angle measured from the Cu(220) DF images. This interface structure remains during the oxide growth, as revealed by measuring pyramids with different lateral sizes. The surface topology obtained from atomic force microcopy (AFM) reveals that the pyramids have a hollow structure, and the terraces and ledges are present along the outer and inner walls of the pyramids as shown in Figs. 3(a) and 3(b). The ledge height along the pyramid wall is measured to be ~55 nm from the AFM images.

It is assumed that the formation of these peculiar terraced-hollow pyramids is related to the generation of compressive stress in the oxide. It has been revealed that oxidation of Cu films results in three-dimensional (3D) growth of oxide islands [7,8], i.e., the islands embed into Cu substrate as growth proceeds. This has been confirmed by thermal reduction of oxide islands formed on Cu(100) surface, which leave behind indentations on Cu surfaces [6]. It is expected that the oxide islands completely penetrate through the 70 nm-thick Cu film very quickly for the oxidation at 900 °C. The oxide growth creates compressive stress in the island due to the large volume increase (~60%) accompanied with the conversion of Cu to Cu_2O. This compressive stress first causes lattice distortions in the oxide, as known from the HREM observation [Fig. 2(f)]. With the continuous formation of new Cu_2O at the metal-oxide interface, this stress increases progressively, and finally causes plastic slips inside the oxide to release the stress. As a result, the central part of the island is squeezed out, leading to the hollow space inside the pyramid and the terraces and ledges along the outer and inner walls. The ledge height is determined by the extent of the relaxation of the total compressive stresses, and the terrace width is determined by the shear stress required for the slip. This process of buildup of the compressive stress by oxide growth, and release of the stress by plastic slip, repeats itself during the pyramid growth, leading to the

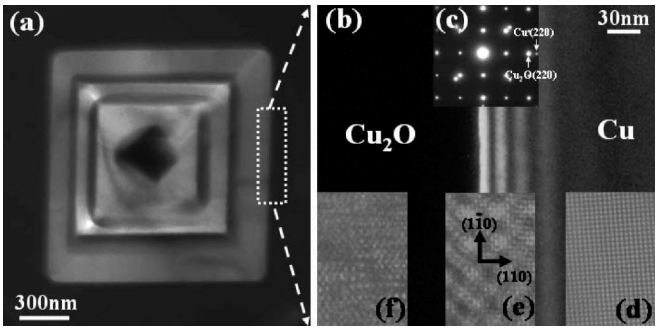

FIG. 2. TEM analysis of the microstructure at the Cu/Cu_2O interface. (a) A terraced Cu_2O pyramid; (b) Cu(220) DF TEM micrograph showing the Cu_2O/Cu interface from the framed area in (a); (c) electron diffraction pattern from the interface area; (d) HREM image of Cu lattice away from the interface; (e) HREM image from the interface area; (f) Cu_2O lattice image away from the interface.

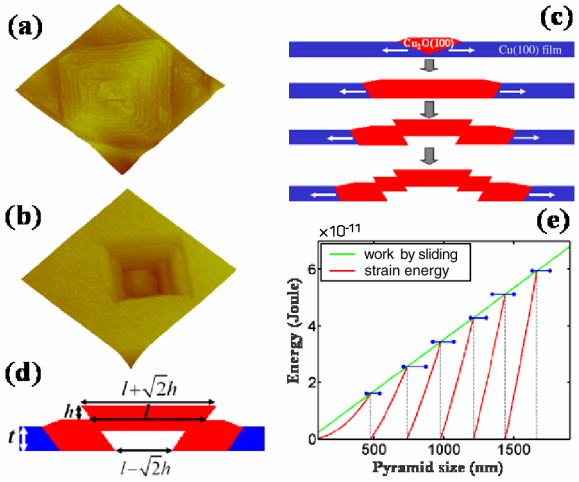

FIG. 3 (color online). (a) AFM image (2 μm × 2 μm, z range: 0.5 mm) of a Cu_2O pyramid from top-down view; (b) AFM image (2 μm × 2 μm, z range: 0.4 μm) of a Cu_2O pyramid from bottom-up view; (c) the proposed plastic-slip mechanism for the formation of the terraced-hollow pyramid, where the white arrows represent lateral growth of the pyramid; (d) structural parameters of the terraced pyramid; (e) plot of the strain energy and the work done by slip, where their intersections correspond to the island sizes at which plastic slips occur, the error bars represent the ranges of terrace widths obtained from experimental measurements of different pyramids.

formation of the hollow pyramids with multiple terraces and ledges, as schematically shown in Fig. 3(c).

The proposed model provides a simple mechanical explanation for the creation of this unusual hollow pyramid structure. We can calculate the strain energy of an oxide island before the first slip as,

$$E_s = \frac{1}{3}t\left(\frac{E}{1-\nu}\varepsilon^2\right)(3l^2 - 3\sqrt{2}tl + 2t^2), \qquad (1)$$

where E, ν is Young's modulus and the Poisson ratio of Cu_2O; respectively, $\varepsilon = \frac{a_{Cu_2O} - a_{Cu}}{a_{Cu}}$ corresponds to the length constraint caused by the lattice change from Cu to Cu_2O, and l and t are the size parameters of the pyramid as defined in Fig. 3(d). The oxide growth causes progressive accumulation of strain energy in the island, and the strain energy is finally released by the plastic slip at some critical lateral size of the island. The work done by slip process can be calculated as

$$W = 3\tau l[t^2 - (t-h)^2] - \sqrt{2}\tau[t^3 - (t-h)^3], \qquad (2)$$

where τ is the shear stress required for the plastic slip in the pyramid, and the size parameters are the same as defined in Fig. 3(d). The hollowing process by the slip creates new inner and outer surfaces and as a result, extra surface energies. The total extra surface energy created during the hollowing process is estimated as $\sim 5 \times 10^{-13}$ J by considering the total new surface area. In comparison, the strain energy obtained from Eq. (1) is $\sim 1.7 \times 10^{-11}$ J. Therefore, the extra surface energy is small compared with the strain energy, and we simply consider that the strain energy is completely released by the slip. Thus, the shear stress for the slip is estimated to be 2.5 GPa by equating Eqs. (1) and (2) and using an experimentally determined width (~ 560 nm) and height (~ 55 nm) of the first terrace and ledge.

The strain energy and work done by slip for the formation of multiple terraces can be calculated, respectively, as

$$E_S^i = t[(l_i^2 - l_{i-1}^2) - \sqrt{2}t(l_i - l_{i-1})]\left(\frac{E}{1-\nu}\right)\varepsilon^2, \qquad i \geq 2, \qquad (3)$$

$$W^i = 3\tau l_i[t^2 - (t-h)^2] - \sqrt{2}\tau[t^3 - (t-h)^3], \qquad (4)$$

where h, t, E, ν, ε have the same definition as Eq. (1) and (2), l_i, l_{i-l} is the island lateral size for the ith and (i-l)th terrace, respectively. Figure 3(d) shows the calculated strain energy and the work done by the slip, and their intersections correspond to the island lateral size at which slips occur. In our analysis, only one fit parameter, i.e., the critical shear stress for slip to occur, is used, and a quite good fit is noted between the experimental island dimensions and the theoretical island dimensions, as shown in Fig. 3(d), where the terrace widths measured from different pyramids are given.

From this analysis, it is known that the compressive stress provides the driving force for slips in the oxide pyramid, and the determined shear stress for the slip is 2.6 GPa. This stress is very high and close to the theoretical strength (~ 3.5 GPa) of Cu_2O. In metals, the deformation shear stresses are often several orders of magnitude less than theoretical strength due to the existence of localized structural defects. The experimental data regarding Cu_2O deformation is not readily available in the literature, however, in ceramics materials, slip by dislocation motion is more difficult than metals, this is because ions of like charge have to be brought into close proximity of each other, i.e., larger barrier for dislocation motion, and the dislocations are often inactive at stresses below the fracture stress [9]. On the other hand, the stress required for deformation increases significantly as the dimensions of materials approach to nanoscale [10,11]. Therefore, the shear stress to start slip in the Cu_2O pyramids can be high.

Clearly, the formation of the terraced-hollow pyramids depends on the mechanical properties of the oxide and the metal films. The Young's modulus (E) and shear modulus (G) of Cu_2O is ~ 30 GPa and ~ 10 GPa, respectively, which is smaller than that of copper ($E = 124$ GPa, $G = 40$ GPa), even considering their temperature dependence [12]. On the other hand, the Cu thin films are annealed at $\sim 900\,^\circ$C before oxidation. This procedure is effective to eliminate any preexisting dislocations in the film. Therefore, the Cu films are dislocation free before oxidation, as confirmed by our *in situ* TEM observation. The higher mechanical modulus of the Cu film and absence of preexisting dislocations in the Cu film drive the oxide pyramids to release the strain, rather than by the Cu film itself.

The calculation from Eqs. (1)–(4) reveals that the structure of the terraced pyramids, such as terrace width and ledge height, is closely related to the mechanical properties of the oxide and metal film, and physical dimensions of the metal films. These dependences allow us to control the pyramid structure. For example, we can change the structural features of the pyramids by changing the thickness of Cu films. Figure 4 shows the oxidation of Cu films with different thickness, where the feature size of the pyramids

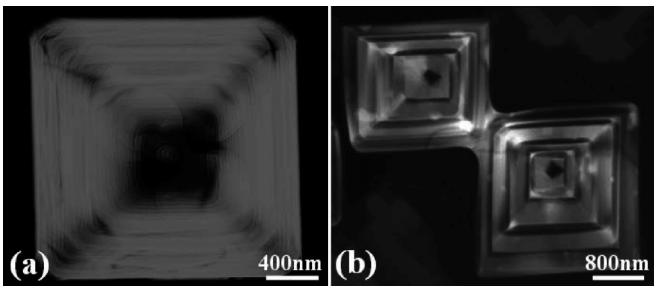

FIG. 4. The terraced-hollow pyramids obtained by oxidizing Cu films with different thickness (a) 50 nm; (b) 90 nm. Oxidation of the thinner/thicker Cu film results in pyramids with smaller/larger terrace width and ledge height.

for 50 nm-thick Cu film is ~380 nm (lateral size corresponding to the first slip), ~65 nm (terrace width), and ~35 nm (ledge height), respectively; and ~640 nm, ~160 nm, and ~68 nm for the 90 nm-thick Cu film, consistent with the model prediction.

In conclusion, terraced-hollow oxide pyramids are formed during oxidation of Cu(001) thin films at ~900 °C. A simple mechanical mechanism, instead of the kinetic/thermodynamic mechanism that is typically used to describe nanostructure evolution, is proposed to explain the formation of this novel structure. Island formation during oxidation has been observed in many other metal systems, such as Ni, Fe, Ti, Co, Pd, Ir, Sn, as well as in Cu [3,4,13–18]. By carefully choosing the oxidation conditions such as the oxygen partial pressures and the oxidation temperatures, it is reasonably expected that the similar terraced-hollow oxide pyramids may be realized in these metal systems and these peculiar structures may have potential applications in development of nanodevices.

This project is funded by the National Science Foundation (NSF DMR No. 9902863) and a National Association of Corrosion Engineers (NACE) seed Grant. The experiments were performed at the Materials Research Laboratory, University of Illinois at Urbana-Champaign, which is supported by the U.S. Department of Energy (No. DEFG02-96-ER45439). We thank J. Wiezorek, I. Nettleship, L. Wang, D. Wolf, R. McAfee, W. Dai, R. Ding, and L. Li for the helpful discussions and suggestions.

*Present address: Materials Science Division, Argonne National Laboratory, IL 60439, USA.

[1] H. E. Evans, Int. Mater. Rev. **40**, 1 (1995).
[2] P. Hancock and R. C. Hurst, in *Advances in Corrosion Science and Technology*, edited by R. W. Staehle and M. G. Fontana (Plenum, New York, 1974), p. 1.
[3] S. Aggarwal, A. P. Monga, S. R. Perusse, R. Ramesh, V. Ballarotto, E. D. Williams, B. R. Chalamala, Y. Wei, and R. H. Reuss, Science **287**, 2235 (2000).
[4] S. Aggarwal, S. B. Ogale, C. S. Ganpule, S. R. Shinde, V. A. Novikov, A. P. Monga, M. R. Burr, R. Ramesh, V. Ballarotto, and E. D. Williams, Appl. Phys. Lett. **78**, 1442 (2001).
[5] M. L. McDonald, J. M. Gibson, and F. C. Unterwald, Rev. Sci. Instrum. **60**, 700 (1989).
[6] G. W. Zhou and J. C. Yang, Phys. Rev. Lett. **93**, 226101 (2004).
[7] J. C. Yang, M. Yeadon, B. Kolasa, and J. M. Gibson, Appl. Phys. Lett. **70**, 3522 (1997).
[8] G. W. Zhou and J. C. Yang, Appl. Surf. Sci. **222**, 357 (2004).
[9] T. Suzuki, S. Takeuchi, and H. Yoshinaga, *Dislocation Dynamics and Plasticity* (Springer-Verlag, Berlin, 1985).
[10] R. W. Siegel and G. E. Fougere, Nanostruct. Mater. **6**, 205 (1995).
[11] M. J. Mayo, Nanostruct. Mater. **9**, 717 (1997).
[12] H. J. Frost and M. F. Ashby, *Deformation-Mechanism Maps* (Pergamon, Oxford, 1982).
[13] K. Thurmer, E. Williams, and J. Reutt-Robey, Science **297**, 2033 (2002).
[14] G. W. Zhou and J. C. Yang, Phys. Rev. Lett. **89**, 106101 (2002).
[15] E. E. Hajcsar, P. R. Underhill, and W. W. Smeltzer, Langmuir **11**, 4862 (1995).
[16] P. H. Holloway and J. B. Hudson, Surf. Sci. **43**, 123 (1974).
[17] P. Marikar, M. B. Brodsky, C. H. Sowers, and N. J. Zaluzec, Ultramicroscopy **29**, 247 (1989).
[18] S. R. Shinde, A. S. Ogale, S. B. Ogale, S. Aggarwal, V. A. Novikov, E. D. Williams, and R. Ramesh, Phys. Rev. B **64**, 035408 (2001).